
Modelling the Flow Structure in Local Scour Around Bridge Pier

USMAN GHANI*, SHAHID ALI**, AND ABDUL GHAFAR***

RECEIVED ON 26.03.2013 ACCEPTED ON 05.06.2013

ABSTRACT

Bridge pier scouring is an important issue of any bridge design work. If it is not taken into account properly, then results will be disastrous. A number of bridges have failed due to clear water local scouring of piers. This research paper presents a numerical model study in which an attempt has been made to explore the flow variables which exist in and around a scoured bridge pier. A finite volume based model of bridge pier was developed using 3D (Three Dimensional) numerical code FLUENT and GAMBIT. After validation process, different discharge values were considered and its impact on three dimensional characteristics of flow such as stream-wise velocities on longitudinal and transverse sections, turbulence circulation cells, and boundary shear stresses was investigated. It was observed that increasing the discharge results in more turbulence around the pier on its downstream side and turbulence properties are intensified in such a situation. However, the primary velocities on the downstream side remain almost unchanged. The results have been presented in the form of contours, vector of primary velocities and x-y plots of bed shear stresses. This study can be used for enhanced understanding of flow features and improvement of formulae for prediction of scour holes around piers.

Key Words: Pier Scour, Open Channel, Boundary Shear Stresses, Navier-Stokes Equations, FLUENT.

1. INTRODUCTION

Scouring around a bridge pier is a common phenomenon and results in huge disasters. It has been observed that approximately 60% of the bridges around the globe fail due to hydraulic related problems. One of the main causes of the bridge failure is the scouring process which happens around the piers of the bridge when there is no inflow of sediments. This situation is normally termed as clear water local scour. In such a situation the scour which happens around the vicinity of the pier is not refilled during the recession of the discharge because there will be no inflow of the

sediments. This is opposite to live bed local scour in which locally scoured bridge pier is refilled after recession of the flood discharge.

When the approaching water encounters a bridge pier, it generates large scale vortices. A lot of turbulence is also created during this process which causes the erosion and transport of sediment in the vicinity of the pier structure. The scouring process keeps on developing till an equilibrium stage is reached. A lot of studies of bridge pier scouring take this equilibrium scoured hole as an

* Assistant Professor, Department of Civil Engineering, University of Engineering & Technology, Taxila.

** Senior Engineer, Pakistan Atomic Energy Commission, Islamabad.

*** Professor, Quaid-e-Azam College of Technology, Sahiwal.

input and then investigate the flow features in this scoured hole.

A number of researchers have carried out experimental and field research work in this area. Karim and Kamil, [1-2] carried out research for exploring the flow features around a pier using numerical modeling and tried to understand different flow characteristics. Similarly Tarek, et. al. [3] used numerical technique to understand flow behavior in a scoured bridge pier. Kirkil, et. al., [4] used detached eddy simulation technique to understand the flow behavior in a bridge pier scouring. There are also studies regarding the temporal variation of bridge pier [5-6]. Chrisohoides, et. al., [7] studied coherent flow structure in a flat abutment using both numerical and computational fluid dynamics technique. Similarly Dehghani, et. al., [8] conducted clear water local scouring using three dimensional numerical code. Khosronejad, et. al., [9] did experimental work on bridge pier scouring. They also simulated their own data to further enhance the flow features under three different pier shapes. Originally it was done for circular and then simulated for square and prism shapes. Chreties, et.al., [10] made experimentation on different pier groups.

This paper presents a numerical simulation work of flow field around a bridge pier after scouring process. The features which were investigated included primary velocities and boundary shear stresses. Three dimensional computational technique has been used for this purpose.

2. VARIOUS NUMERICAL PARAMETERS OF THE PIER SCOUR MODEL

The bridge pier scouring model was set up using a 3D numerical code FLUENT. It is based on three dimensional continuity and Navior-Stokes equations which can be summarized as:

Continuity Equation

$$\frac{\partial U_i}{\partial x_i} = 0 \quad (1)$$

The three dimensional Navior -Stokes equations are as:

$$\frac{\partial(\rho u)}{\partial t} + \frac{\partial(\rho u^2)}{\partial x} + \frac{\partial(\rho uv)}{\partial y} + \frac{\partial(\rho uw)}{\partial z} = -\frac{1}{\rho} \frac{\partial p}{\partial x} + \rho f_x + \mu \left(\frac{\partial^2 u}{\partial x^2} + \frac{\partial^2 u}{\partial y^2} + \frac{\partial^2 u}{\partial z^2} \right) \quad (2)$$

$$\frac{\partial(\rho v)}{\partial t} + \frac{\partial(\rho vu)}{\partial x} + \frac{\partial(\rho v^2)}{\partial y} + \frac{\partial(\rho vw)}{\partial z} = -\frac{1}{\rho} \frac{\partial p}{\partial y} + \rho f_y + \mu \left(\frac{\partial^2 v}{\partial x^2} + \frac{\partial^2 v}{\partial y^2} + \frac{\partial^2 v}{\partial z^2} \right) \quad (3)$$

$$\frac{\partial(\rho w)}{\partial t} + \frac{\partial(\rho wu)}{\partial x} + \frac{\partial(\rho wv)}{\partial y} + \frac{\partial(\rho w^2)}{\partial z} = -\frac{1}{\rho} \frac{\partial p}{\partial z} + \rho f_z + \mu \left(\frac{\partial^2 w}{\partial x^2} + \frac{\partial^2 w}{\partial y^2} + \frac{\partial^2 w}{\partial z^2} \right) \quad (4)$$

The Reynolds -Averaged Navior Stokes equations are as follows:

$$\frac{\bar{u}(\bar{\partial u})}{\partial x} + \bar{v} \frac{\partial \bar{u}}{\partial y} + \bar{w} \frac{\partial \bar{u}}{\partial z} = -\frac{1}{\rho} \frac{\partial \bar{P}}{\partial x} + u \left(\frac{\partial^2 u}{\partial x^2} + \frac{\partial^2 u}{\partial y^2} + \frac{\partial^2 u}{\partial z^2} \right) - \left(\frac{\partial \overline{u'u'}}{\partial x} + \frac{\partial \overline{u'v'}}{\partial y} + \frac{\partial \overline{u'w'}}{\partial z} \right) \quad (5)$$

$$\frac{\bar{u}(\bar{\partial v})}{\partial x} + \bar{v} \frac{\partial \bar{v}}{\partial y} + \bar{w} \frac{\partial \bar{v}}{\partial z} = -\frac{1}{\rho} \frac{\partial \bar{P}}{\partial y} + u \left(\frac{\partial^2 v}{\partial x^2} + \frac{\partial^2 v}{\partial y^2} + \frac{\partial^2 v}{\partial z^2} \right) - \left(\frac{\partial \overline{u'v'}}{\partial x} + \frac{\partial \overline{v'v'}}{\partial y} + \frac{\partial \overline{v'w'}}{\partial z} \right) \quad (6)$$

$$\frac{\bar{u}(\bar{\partial w})}{\partial x} + \bar{v} \frac{\partial \bar{w}}{\partial y} + \bar{w} \frac{\partial \bar{w}}{\partial z} = -\frac{1}{\rho} \frac{\partial \bar{P}}{\partial z} + u \left(\frac{\partial^2 w}{\partial x^2} + \frac{\partial^2 w}{\partial y^2} + \frac{\partial^2 w}{\partial z^2} \right) - \left(\frac{\partial \overline{u'w'}}{\partial x} + \frac{\partial \overline{v'w'}}{\partial y} + \frac{\partial \overline{w'w'}}{\partial z} \right) \quad (7)$$

where P is the pressure, ν and ρ are the kinematic viscosity and density of the water, u, v, w are instantaneous velocities in x, y, z directions, t is time, f_x, f_y, f_z are body forces, the over bar indicates the average of all the instantaneous components, $u_p u_j$ are the Reynolds stresses which result from the decomposition of instantaneous velocities into their mean and fluctuating components.

First of all, the model was validated against the available experimental data from the literature. A brief description of the data is as follows. Sarker, [11] performed experiments at the Coastal and Offshore Engineering Institute, University of Malaysia. The experimental set-up was comprised of a re-circulating flume of length 16.10 m, width 0.90 m and a total height of 0.72 m. The flume was supported by a steel frame. It was comprised of tanks, pumps, sump and pipe network. For experimental work, a bed made of plywood was placed on the bottom of the flume. Sediment size used for preparation of the bed was ranged from 0.42-2.0mm. The diameter of the pier was 0.89 m. The velocity measurements were taken with three dimensional acoustic doppler velocimeter.

The mesh generator available with FLUENT 12 i.e. GAMBIT 2.3 has been used for meshing the physical domain. The unstructured mesh comprising of triangular elements was used for this purposes. The paving scheme was used for the meshing process. The mesh has been shown in Fig. 1. The simulated results for primary velocity were compared with experimental data as shown in Fig. 2. It was observed that the predictions by the numerical model are reasonably good and the simulated results match the experimental data. The mesh independence was achieved by doubling the meshes in longitudinal, lateral and vertical directions. It was observed that the mesh finally used for simulation purposes can be categorized as mesh independent. The difference in results of this mesh with a further refined mesh is less than 1%. The mesh

independence results have been shown in Fig. 3. The node numbers for Mesh 1, Mesh 2 and Mesh 3 are 100x40x25, 200x80x50 and 400x160x100 respectively. The finally used mesh was 100x40x25. The mesh independence test was performed for stream-wise velocity values (x-velocity). The mesh was made dense in the vicinity of the bridge pier whereas it was gradually coarsened as we moved away from the pier. This is because the steep change of properties occurs in this region.

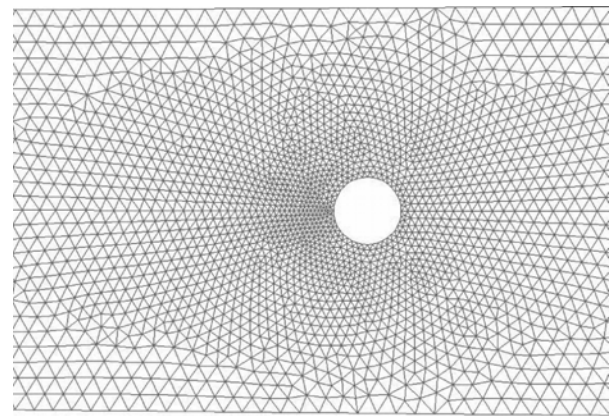


FIG. 1. MESH USED IN THE SIMULATION

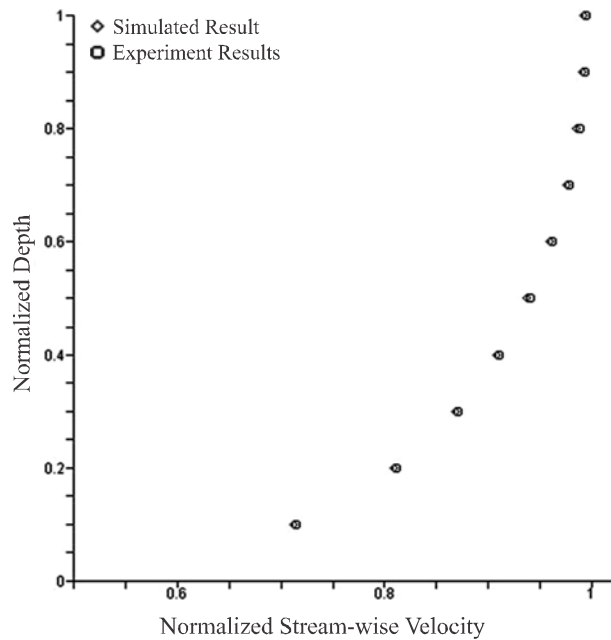


FIG. 2. GRAPH SHOWING VALIDATION OF RESULTS

It is essential that values of different variables be given at the boundaries of the selected flow domain before conducting any numerical simulation work. This serves as the input data based upon which simulation is

performed and the results are calculated. In this study, the velocity values were provided at the inlet as a boundary condition, zero gauge pressure (atmospheric pressure) was taken at the exit of the flow domain, a no slip boundary condition was given at the bed and side walls. At the free surface, a free slip wall boundary condition with zero shear stress was assumed. The turbulence model selected was Reynolds stress model. The other important numerical parameters include; SIMPLE (Semi Implicit Method for Pressure Linked Equations) algorithm for pressure velocity coupling, second order upwind schemes for different conservation equations, 1×10^{-6} as convergence limit and Reynolds stress model for closure purposes.

The simulation process will stop once convergence will reach. The Fig. 4 shows the convergence history for the modeling. It indicates that convergence criteria were reached much earlier for momentum equations than continuity equations. The total iterations for this simulation were 6,273.

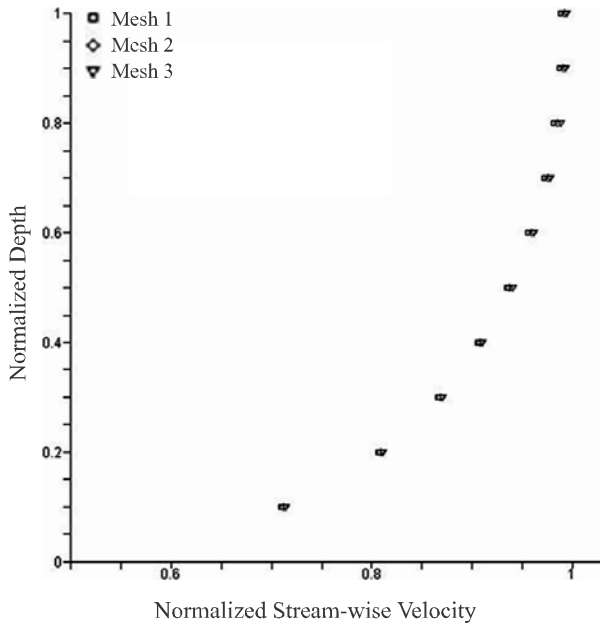


FIG. 3. MESH INDEPENDENCE RESULTS

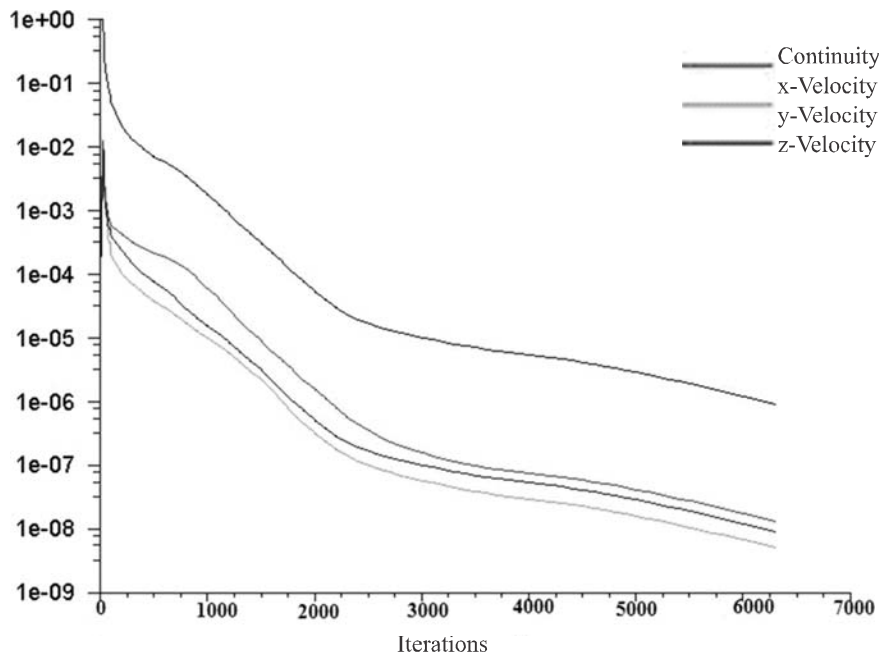


FIG. 4. CONVERGENCE HISTORY OF DIFFERENT VARIABLES OBTAINED DURING MODELING

3. RESULTS AND DISCUSSION

This paper presents the flow characteristics in a scoured bridge pier. The characteristics which are important in this study are primary and secondary velocity values along with the bed shear stresses. The variables have their impact on pier scouring and having a clear understanding of these things will result in design improvement and rehabilitation of the pier scour works. The Fig. 5 represents the primary velocity at the free surface. The flow direction is from right to left of the Fig. Fig. 5 shows that the velocity values are high upstream the pier and these are maximum on the sides of the pier, however then there is a sudden drop of velocities just behind the bridge pier and velocities turn to zero or move into negative range in that portion. This has been captured by the existing numerical model. The velocities on locations away from the pier remain almost unchanged. This means that major influence of pier is in its vicinity.

Fig. 6(a-c) below represents the primary velocity contours at a section 0.5m upstream the pier. Three different discharge values considered in this simulation work are 30, 35 and 40 litre/sec. It has been observed through these diagrams that increasing discharge values have considerably changed the primary velocities especially in the regions of pier.

In this region the difference of velocity from low to high discharge is approximately 12-15%. However, this difference is less prominent in rest parts of the cross-section.

Fig. 7 depicts the primary velocity distribution at a section passing through the pier. As is clear from this diagram, the velocity values are zero in the region of pier. This has been captured successfully by the numerical model. However, these are very high adjacent to the pier as shown by the contour diagram.

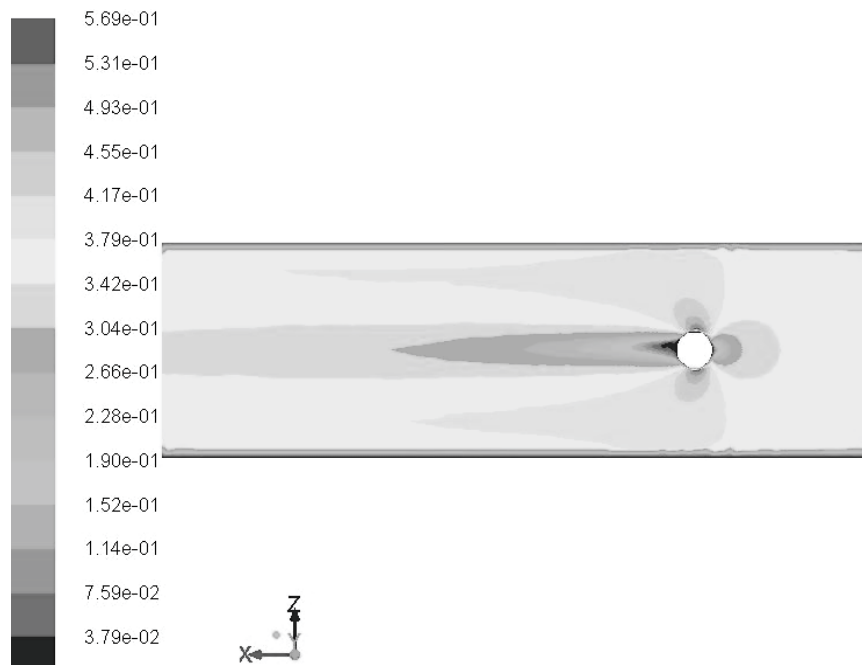


FIG. 5. PRIMARY VELOCITY CONTOURS AT A LONGITUDINAL SECTION OVER THE FREE SURFACE

Fig. 8(a-c) shows the velocity distributions at a section 0.5m downstream of the pier. In Fig. 8(a-c) it is clear that the impact of fluctuating discharge on velocities is more prominent as compared to the upstream side. This might

be attributed to the fact that there is horse-shoe vortex phenomenon existing on the downstream side which might be controlling the impact of varying discharge on flow values. Again just like the upstream side, the impact of

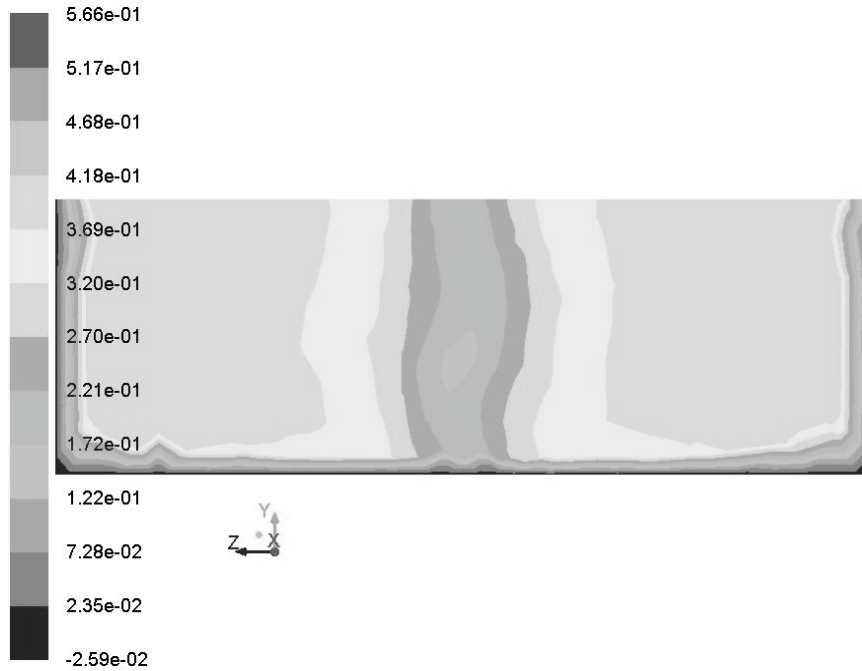


FIG. 6(a). PRIMARY VELOCITY CONTOURS AT A CROSS-SECTION UPSTREAM THE PIER FOR LOW DISCHARGE

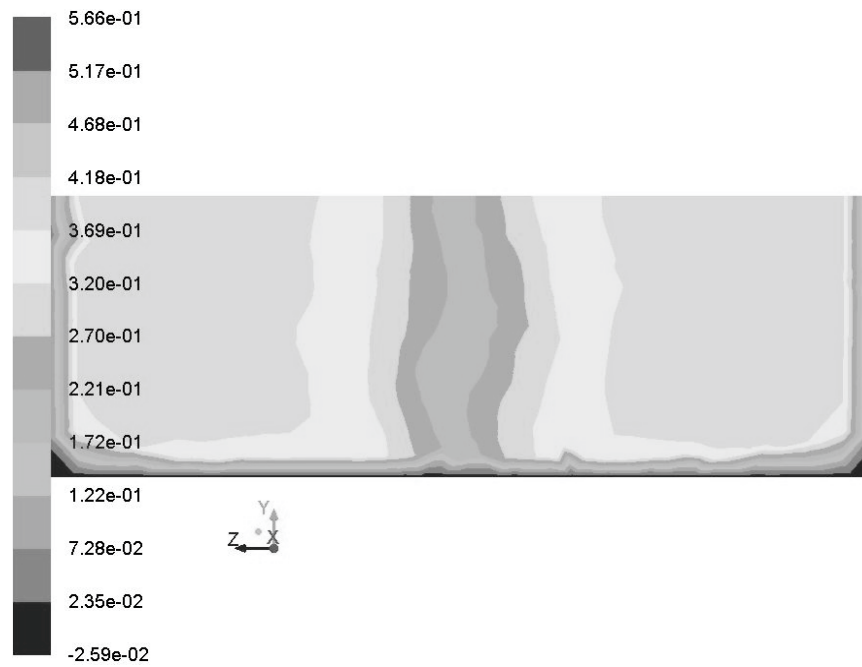


FIG. 6(b). PRIMARY VELOCITY CONTOURS AT A SECTION UPSTREAM THE PIER FOR MEDIUM DISCHARGE

discharge is more in the vicinity and just behind the pier whereas it has less impact on other regions of the cross-section. This has been observed in all the three cases of discharge values.

Fig. 9 represents the vector plots of primary velocities (stream-wise velocities in the longitudinal direction) existing at the free surface of the channel. As the flow pattern remains same for all the three situations, so

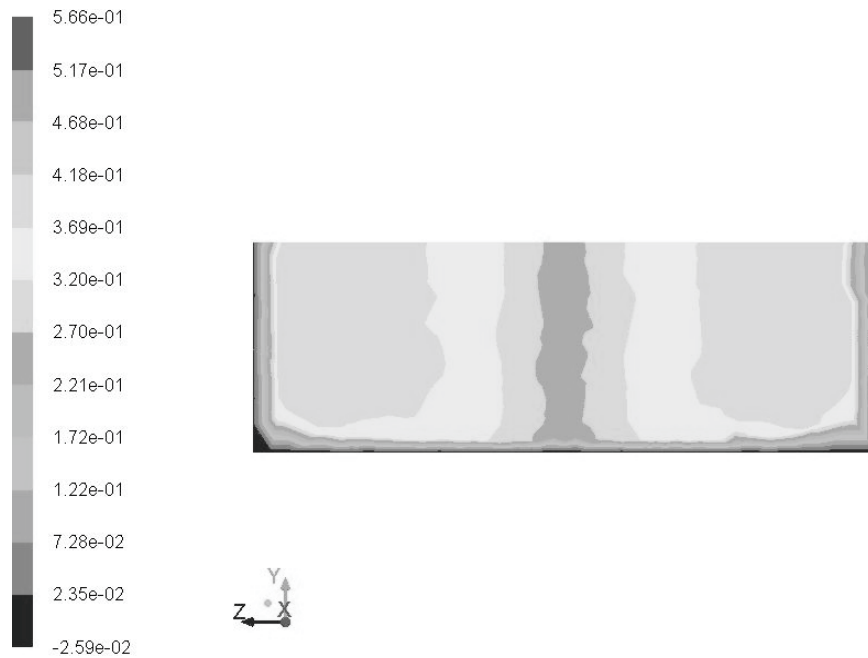


FIG. 6(c). PRIMARY VELOCITY CONTOURS AT A CROSS-SECTION UPSTREAM THE PIER FOR HIGH DISCHARGE

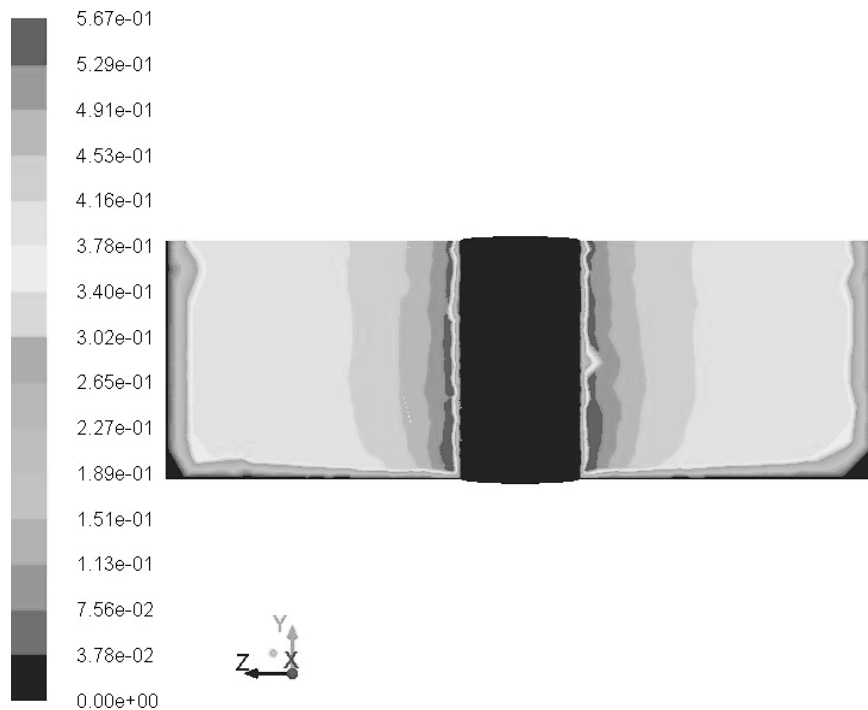


FIG. 7. STREAM WISE VELOCITY CONTOURS OVER A SECTION PASSING THROUGH THE PIER

only one case has been shown in this diagram. It indicates that the velocities are minimum on the downstream side and maximum along the periphery on the sides of the pier. The Fig. 10(a-b) represents the

distribution of bed shear stresses in cross-stream direction at section 0.5m downstream the pier for low (30 litre/sec) and high (40 litre/sec) discharges respectively.

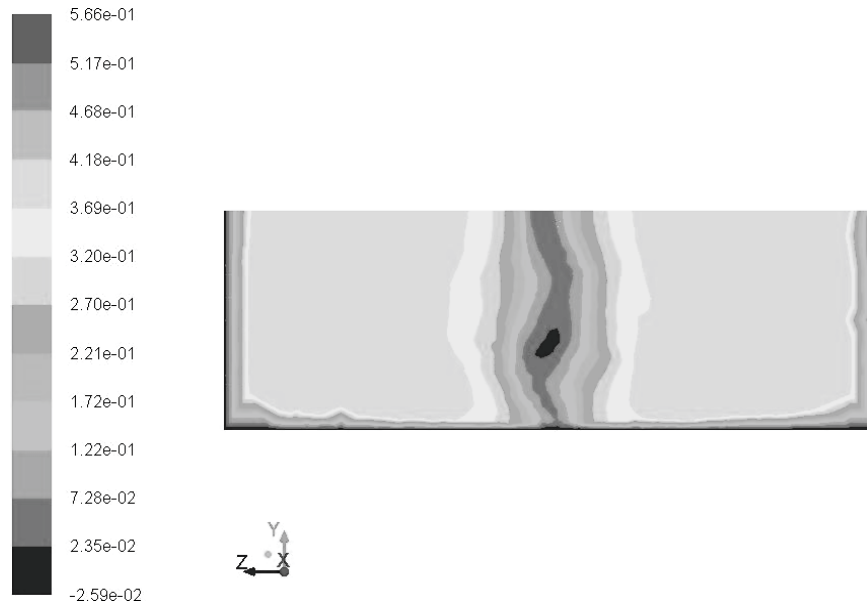


FIG. 8(a). LOW

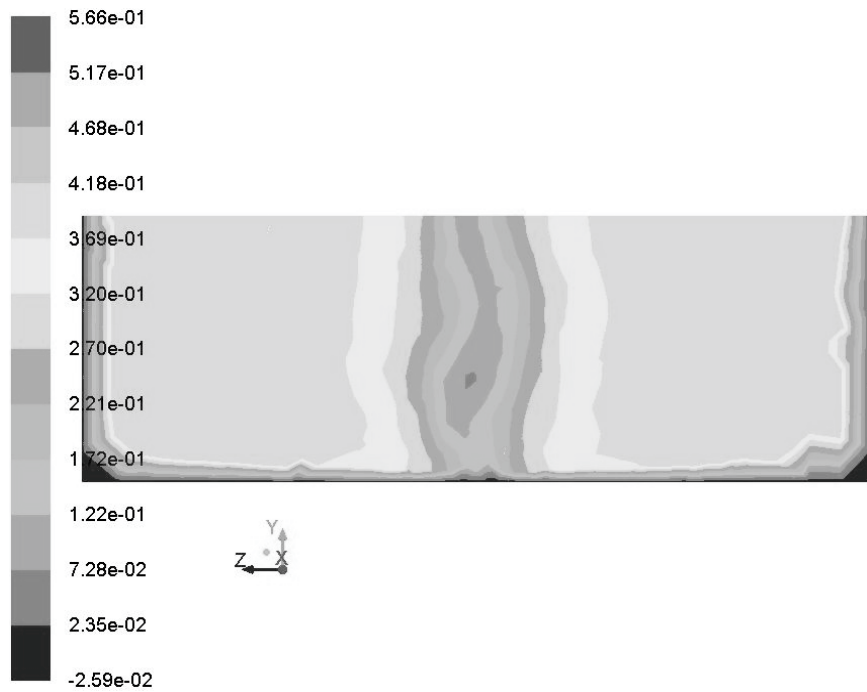


FIG. 8(b). MEDIUM

These diagrams indicate that difference in minimum bed shear stress between low and high discharge cases is almost one fifth. However the maximum bed shear stress intensity has not been affected too much. But the distribution pattern of bed shear stresses remains same for both cases.

The Fig. 11(a-b) indicates the wall shearing stress at upstream and downstream side for high and low discharges. Both the diagrams indicate that the impact of change in discharge intensity is small on these wall shear stresses. The pattern of distribution also remains almost same for the two cases.

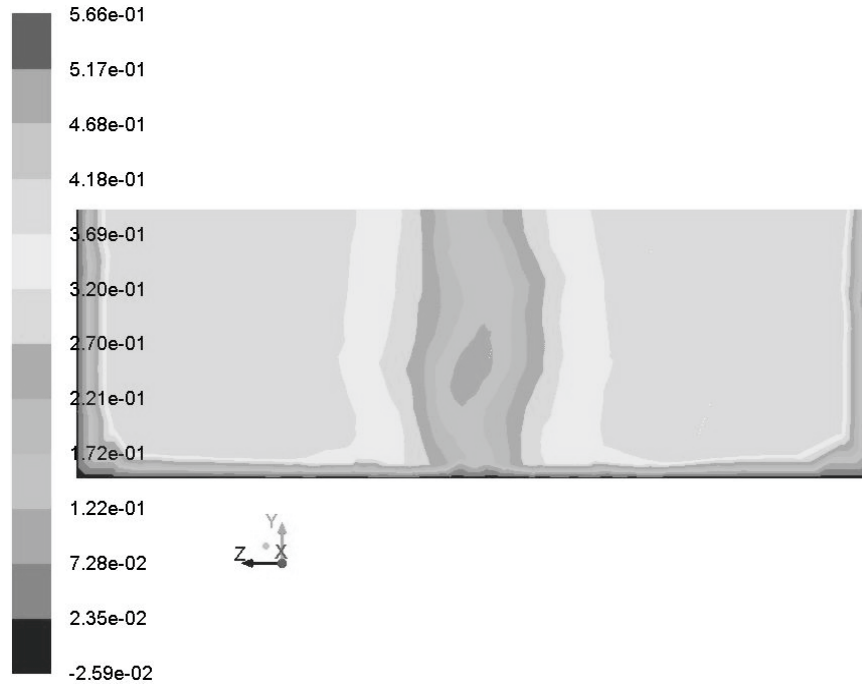


FIG. 8(c). HIGH DISCHARGES
 FIG. 8. PRIMARY VELOCITY CONTOURS AT DOWNSTREAM SECTION

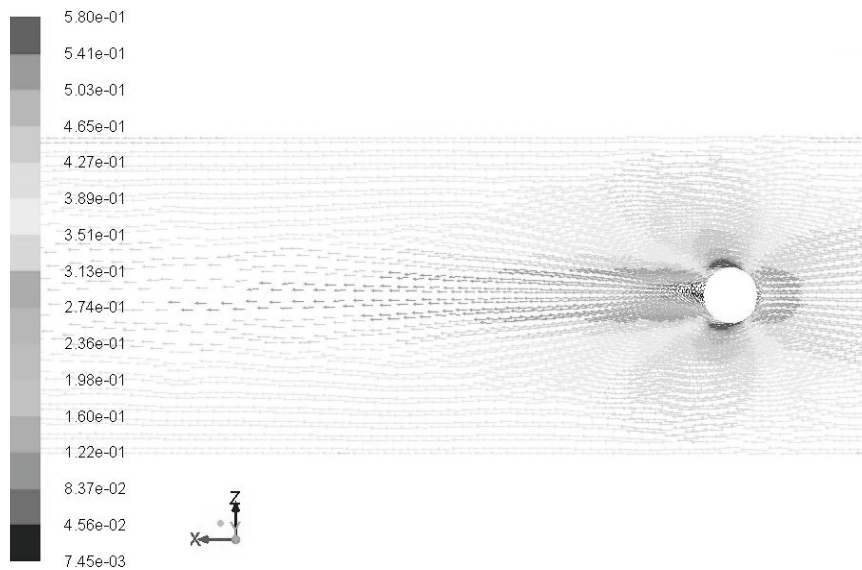


FIG. 9. SECONDARY VELOCITY VECTORS DISTRIBUTED OVER THE FREE SURFACE AROUND THE PIER

4. CONCLUSIONS

A parametric study has been presented in this paper in which the intensity of incoming flow was changed to its impact on different flow features such as primary velocities, bed shear stresses, and wall shear stresses in case of a bridge pier scour. It was observed

that the pattern of primary velocities remain unchanged due to change in discharge values but the cross-stream velocity intensities in central region were much affected at the upstream side and less affected at the downstream side. Also the impact on bed shear stresses was considerable as compared to the wall

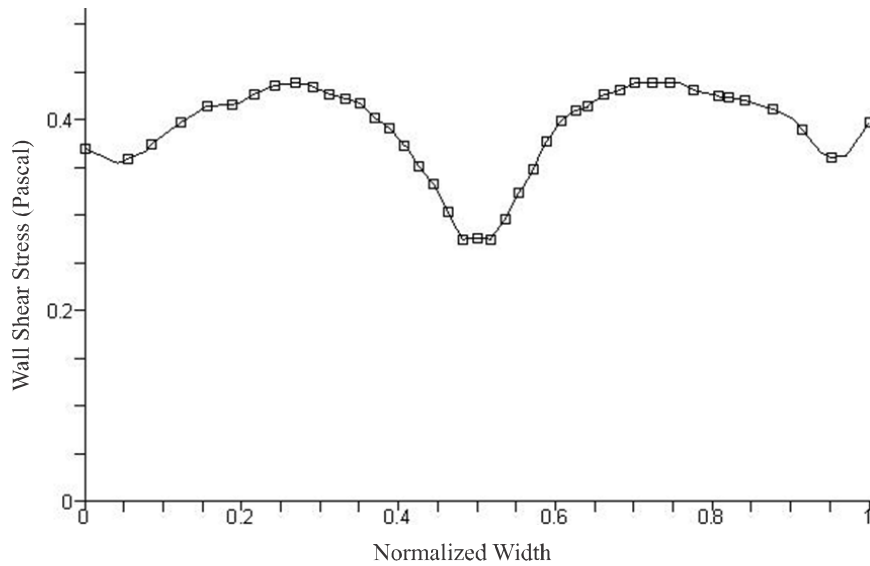


FIG. 10(a). BED SHEARING STRESSES AT A SECTION 0.5M DOWNSTREAM OF PIER FOR LOW DISCHARGE

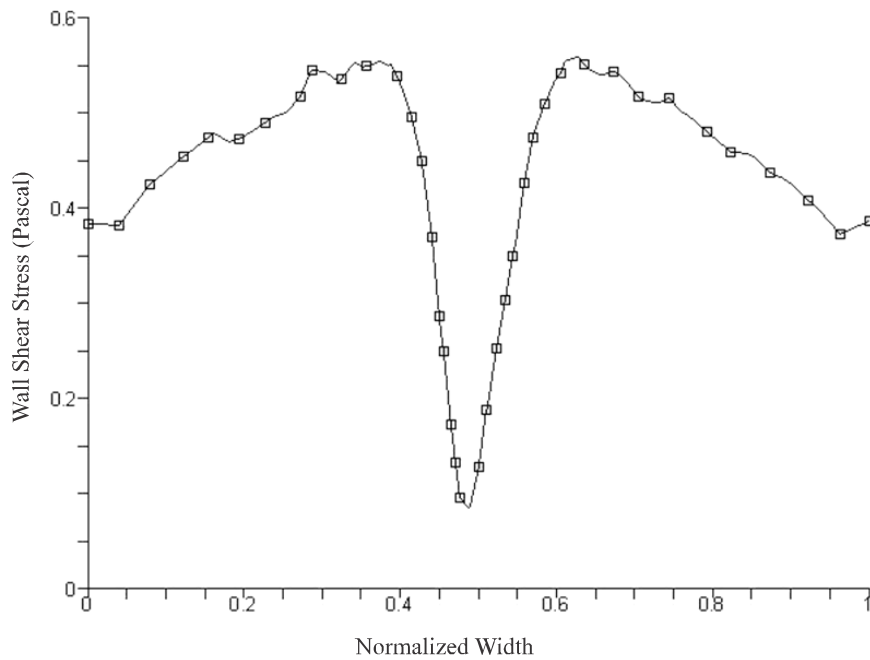


FIG. 10(b). BED SHEARING STRESSES AT A SECTION 0.5M DOWNSTREAM OF PIER FOR HIGH DISCHARGE

shearing stresses. The bed shear stresses varied up to 50% due to the presence of pier. However the pattern

of distribution of these stresses remains unchanged in all the cases.

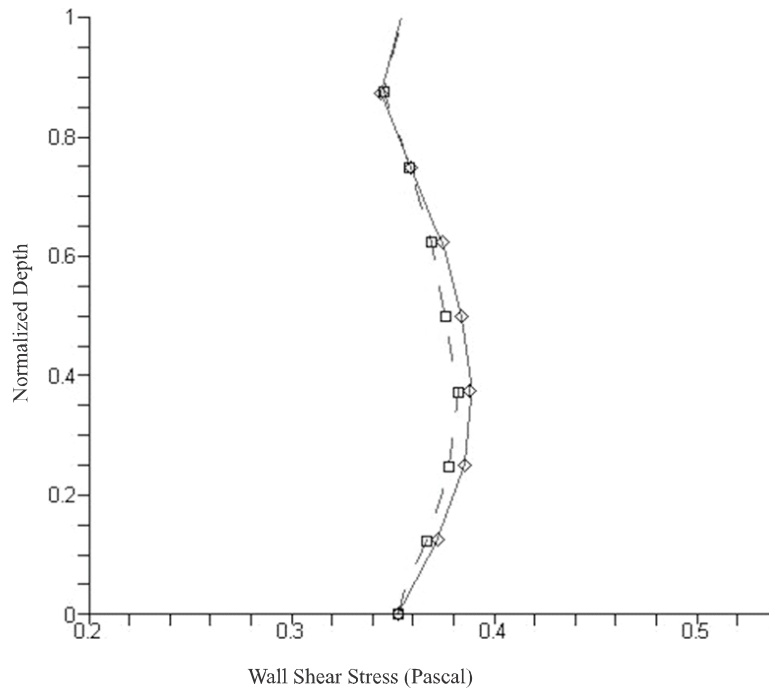


FIG. 11(a). WALL SHEARING STRESSES 0.5M UPSTREAM OF PIER FOR HIGH AND LOW DISCHARGES

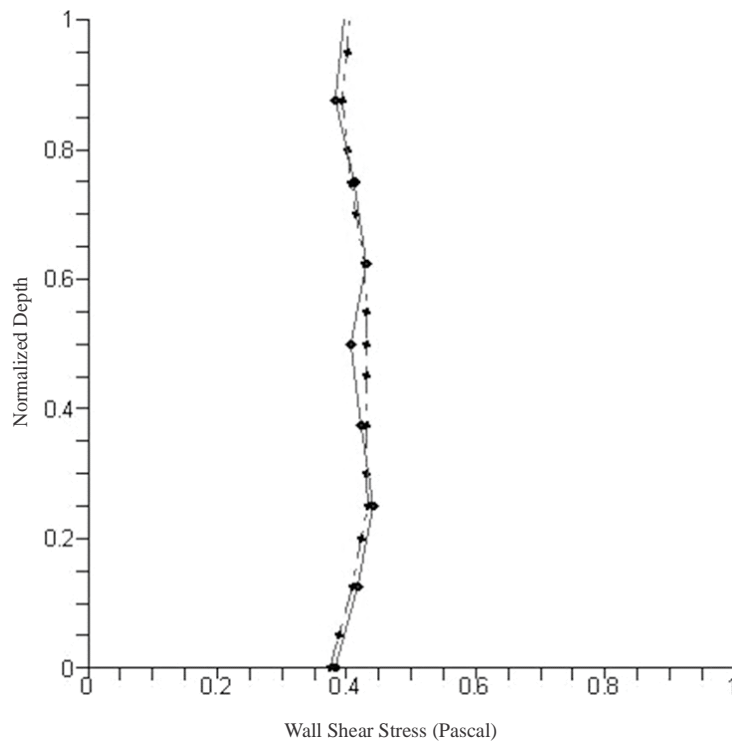


FIG. 11(b). WALL SHEARING STRESSES 0.5M DOWNSTREAM OF PIER FOR HIGH AND LOW DISCHARGES

ACKNOWLEDGEMENTS

The authors are thankful to Higher Education Commission, Pakistan, for providing CFD Software facilities at University of Engineering & Technology, Taxila, Pakistan, which were used to conduct this research work.

REFERENCES

- [1] Karim, O.A., and Ali, K.H.M., "Prediction of Flow Patterns in Local Scour Holes Caused by Turbulent Water Jets", *IAHR Journal of Hydraulic Research*, Volume 38, No. 4, pp. 279-288, Netherland, July, 2000.
- [2] Ali, K.H.M., and Karim, O., "Simulation of Flow Around Piers", *IAHR Journal of Hydraulic Research*, Volume 40, No. 2, pp. 161-174, Netherland, March, 2002.
- [3] Tarek, M.S., Imran, J., and Chaudhry, M.H., "Numerical Modeling of Three Dimensional Flow Field Around Circular Piers", *ASCE Journal of Hydraulic Engineering*, Volume 130, No. 2, pp. 91-100, USA, February, 2004.
- [4] Kirkil, G., Constantineascu, G., and Ettema, R., "Detached Eddy Simulation Investigation of Turbulence at a Circular Pier with a Scour Hole", *ASCE Journal of Hydraulic Engineering*, Volume 135, No. 11, pp. 888-901, USA, November, 2009.
- [5] Mohammadpour, R., Ghani, A.A., and Azamathulla, H.M., "Prediction of Equilibrium Scour Time Around Long Abutments", *Proceeding of ICE Water Management*, Volume 169, pp. 131-142, UK, 2012.
- [6] Yanmaz, A.A., and Altinbilek, H.D., "Study of Time Dependent Local Scour Around Bridge Piers", *ASCE Journal of Hydraulic Engineering*, Volume 117, No. 10, pp. 1247-1268, USA, October, 1991.
- [7] Chrisohoids, A., Sotiropoulos, F., and Terry, W.S., "Coherent Structures in Flat Bed Abutment Flows: Computational Fluid Dynamics and Experiments", *ASCE Journal of Hydraulic Engineering*, Volume 129, No. 3, pp. 177-186, USA, March, 2003.
- [8] Denghani, A.H., Esmacili, T., Chang, W.Y., and Denghani, N., "3D Simulation of Local Scour under Hydrograph", *Proceeding of ICE Water Management*, Volume 168, pp. 1-12, UK, 2011.
- [9] Khosronejad, A., Kang, S., and Sotiropoulos, F., "Experimental and Computational Investigation of Local Scour Around Bridge Piers", *Advances in Water Resources*, Volume, 37, No. 1, pp. 73-85, UK, February, 2012.
- [10] Christies, C., Teixeira, L., and Simarro, G., "Influenc of Flow Conditions on Scour Hole Shape for Pier Groups", *Proceeding of ICE Water Management*, Volume 168, pp. 111-122, UK, 2011.
- [11] Sarker, Md. A., "Flow Measurement Around Scoured Bridge using Acoustic-Doppler Velocimeter", *Journal of Flow Measurement and Instrumentation*, Volume 9, pp. 217-227, 1998.